Design Studies for a VUV–Soft X-ray Free-Electron Laser Array*

J. CORLETT, K. BAPTISTE, J. M. BYRD, P. DENES, R. FALCONE, J. KIRZ, W. MCCURDY, H. PADMORE, G. PENN, J. QIANG, D. ROBIN, F. SANNIBALE, R. SCHOENLEIN, J. STAPLES, C. STEIER, M. VENTURINI, W. WAN, R. WELLS, R. WILCOX, A. ZHOLENTS

Lawrence Berkeley National Laboratory, Berkeley, CA, USA

Introduction

Several recent reports have identified the scientific requirements for a future soft X-ray light source [1, 2, 3, 4, 5], and a high-repetition-rate free-electron laser (FEL) facility responsive to them is being studied at Lawrence Berkeley National Laboratory (LBNL) [6]. The facility is based on a continuous-wave (CW) superconducting linear accelerator with beam supplied by a high-brightness, high-repetition-rate photocathode electron gun operating in CW mode, and on an array of FELs to which the accelerated beam is distributed, each operating at high repetition rate and with even pulse spacing. Dependent on the experimental requirements, the individual FELs may be configured for either self-amplified spontaneous emission (SASE), seeded high-gain harmonic generation (HGHG), echo-enabled harmonic generation (EEHG), or oscillator mode of operation, and will produce high peak and average brightness x-rays with a flexible pulse format ranging from sub-femtoseconds to hundreds of femtoseconds. This new light source would serve a broad community of scientists in many areas of research, similar to existing utilization of storage ring based light sources.

To reduce technical risks and construction costs, accelerator research, development, and design studies at LBNL target the most critical components and systems of the facility. We are developing a high-repetition-rate low-emittance electron gun, high quantum efficiency photocathodes, and have embarked on design and optimization of the electron beam accelerator, FEL switchyard, and array of FELs. We continue our work on precision timing and synchronization systems critical for time-resolved experiments using pump-probe techniques.

Scientific requirements for next-generation light sources

The innovation expected from enhanced X-ray sources lies in combining and extending existing knowledge of matter at the atomic scale, with extreme spatial, temporal, and energy resolution. Properties of anticipated new FEL X-ray sources include the ability to reach ultrafast timescales of electron motion around an atom, the spatial scale of the atomic bond, and the energy scale of the bond that holds electrons in correlated motion with near neighbors. These capabilities will allow probing of the microscopic flow of energy and information within materials and thereby support the design and optimization of novel energy conversion systems. In addition, these novel sources have an intensity and brightness needed to observe the subtlest of nature's secrets at these frontier space, time, and energy scales.

While our understanding of the time- and energy-dependent behavior of matter in its ground or natural state is still severely limited, we know even less about excited states. Such states are of key scientific and technological importance, for they typically determine how matter functions during chemical reactions and during physical and biological processes. Excited states of interest

*This work was supported by the U.S. Department of Energy under Contract No. DE-AC02-05CH11231.

span a vast range, being close to the natural (ground or equilibrium, as appropriate) state (as in electronic transport), relatively far from it (photochemical reactions), and very far from it (as in extreme conditions imposed by pressure, radiation, or electric and magnetic fields).

Embedded in these challenges is the exploration of the atomic or nanoscale on the "natural" timescale of atoms, electrons, and spins and on the "operational" timescale that determines function—key in technological applications. There is presently a striking discrepancy between the natural timescales of atomic motion (about 10 fs), spin motion (down to about 1 fs), and electronic motion (down to attoseconds) and the fastest operational timescales (approaching 100 ps). A critical challenge is to pave the way to expand technology into the ultrafast, with five orders of magnitude in improvement down to the intrinsic timescale of charge and spin motions of valence electrons.

In addition to temporal resolution, spatial resolution is also important on both short and longer timescales characteristic of diffusion and displacement, and of sound propagation, for example. Higher coherent flux from future X-ray sources will permit imaging on timescales approaching MHz. This opens the door to scientific discovery in catalysis, deformation, phase nucleation and transformations.

A high-repetition-rate FEL facility

LBNL staff are developing a design concept for a 10-beamline, coherent, soft x-ray FEL array powered by a 2.4-GeV superconducting accelerator operating with a 1-MHz repetition rate. Nominal 1-nC electron bunches are fanned out through a spreader, distributing beams to an array of 10 independently configurable undulators and FEL beamlines with nominal bunch rates up to 100 kHz. The FELs may be seeded by optical lasers to control the X-ray output characteristics or may use self-amplified spontaneous emission (SASE) techniques, including generation of low-charge, high-brightness bunches with intrinsically short duration. Users specify the wavelength, pulse duration, and polarization, so that the 10 simultaneously operating beamlines can be individually optimized for specific experiments, including broad spectral coverage and multiple beam capability. The spectral range is from 10 eV to 1 keV, with harmonics to approximately 5 keV at reduced intensity. The beams are also synchronized with optical lasers or IR and THz sources for pump–probe experiments. Three principal modes of operation are proposed: ultrashort pulse (300 as–10 fs), short pulse (10 fs–100 fs), and high spectral resolution (requiring pulses from 100–500 fs). The spectral bandwidth in each mode is anticipated to approach fundamental transform limits. Other features include the capability to achieve high peak power (~1 GW) for nonlinear optics, control of peak power to reduce sample damage, and high average power (~1 W) for low-scattering-rate experiments. With 10 beamlines, the facility will be capable of serving ~2000 users per year. Table 1 shows performance goals.

Accelerator R&D and design studies

Electron-beam delivery systems

Electron bunches from an injector require elaborate preparation before becoming suitable for use in an FEL. First, acceleration to sufficiently high energy is necessary to generate short-wavelength X-ray pulses. In our baseline design concept, acceleration is provided by twenty 1.3-GHz TESLA-type superconducting rf modules [7] operating in CW mode with 13.5-MeV/m average gradient. In addition, efficient lasing in FELs also requires an electron beam with high

6D brightness $\hat{B}_{6D} = 2I/(\varepsilon_\perp^2 \sigma_E)$, small transverse emittance $\varepsilon_\perp$, and small uncorrelated energy spread σ_E. The beam peak current I at the exit of the injector (of the order of 70 A) is more than an order of magnitude smaller than the 1-kA design target and is enhanced by bunch compression through a magnetic chicane. Bunch compression must be done while preserving a small transverse emittance (a value at the level of 0.8 μm or less is required for efficient lasing at 1-keV photon energy) while a tight demand on the maximum allowable uncorrelated energy spread ($\sigma_E \approx 100$ keV) is posed by the use of seeding techniques for lasing. During transport to the FELs, a number of effects can degrade beam quality and spoil brightness, including transverse and longitudinal space charge, longitudinal wake fields, and coherent synchrotron radiation. We have investigated these effects extensively and devised strategies to tame their impact on the beam. A schematic of the accelerator layout is shown in Figure 1, and details of the machine configuration are provided in [8].

One of the most delicate issues of beam dynamics is control of the microbunching instability [9], which tends to produce electron-beam fragmentation in longitudinal phase space that would prevent successful operation of a seeded FEL. One way to contain the instability is to perform a one-stage bunch compression through a single chicane. Previous studies showed that configurations with two or more bunch compressors consistently display a higher degree of microbunching instability [10]. A second essential measure is to arrange the spreader to be isochronous [11]. However, the most effective means to control the instability is to employ a laser heater [12], which washes out density fluctuations in the electron bunch by increasing its uncorrelated energy spread. Our studies using the IMPACT code [13] and analytical estimate of the microbunching instability based on a linear model [14] show that a laser heater arranged to generate a 5-keV energy spread allows the electron beam to maintain a reasonably smooth density profile through the end of the spreader while keeping the slice uncorrelated energy spread in the beam core below 100 keV (Figures 2 and 3).

FEL design

A number of techniques have been developed for controlling FEL output, including the use of electron beams that are ultrabright, ultrashort-pulse, optically manipulated, or seeded. A leading technique for a seeded FEL in our project is echo-enabled microbunching [15]. Recent studies [16] indicate that using this technique, one can reach X-ray wavelengths in the water window beginning with an optical seed by performing two relatively simple acts of electron-beam manipulation using laser beams. Confidence in this technique is based on previous experience in modulating the electron-beam energy in slicing sources and seeding experiments; additional tests are planned at a number of facilities.

There is strong interest in the scientific community to learn how chemical bonds in molecules form, break, or change using soft X-ray FELs producing sub-femtosecond X-ray pulses [4]. Our studies show that using an FEL, one can possibly prepare two-color pulses of attosecond-scale duration with a precisely controlled time delay to do stimulated X-ray Raman spectroscopy [17] to address these needs; Figure 4 shows simulated output for a two-color FEL [18]. We continue to explore optical manipulation techniques that can provide exquisite control of the X-ray pulse, allowing novel and powerful experimentation opportunities.

The high electron-bunch repetition rate in our machine offers an excellent opportunity for precision electron-beam diagnostics and use of broadband feedback loops. Simulating a wide

variety of jitter sources, we find that feedback systems can reduce electron-bunch arrival-time jitter from 60 to 20 fs, and the electron-bunch energy jitter from 250 to 90 keV.

Photocathode design

Metal cathodes can be robust, but they suffer from poor quantum efficiency (QE), and that the large work function of most metals requires that UV light is needed for excitation. This means that several stages of harmonic generation have to be used from Ti:Sapphire or Yb-based lasers, limiting the repetition rate based on the average power of currently available lasers. A high repetition rate requires high-QE photocathodes that ideally operate in the optical or IR regimes.

We investigated the use of the alkali antimonides, specifically K_2CsSb, as the basis for a high-rep-rate cathode. This material was used previously in photoinjectors, specifically in the Los Alamos–Boeing FEL [19], and achieved good performance at high average current. It was found to be efficient and reproducible in manufacture, but suffered from oxygen and water contamination that reduced QE over time. However, a 30-hr lifetime was achieved in an improved gun design with improved vacuum. The VHF gun design under development at LBNL (see below), with its high conductance and large pumping capacity, is designed to provide much better vacuum than rf guns and should give commensurately longer cathode lifetimes.

The great advantage of the alkali antimonides is that second harmonic light from a Yb (thin disk or fiber) laser can be used, greatly reducing laser complexity. Our present work is focused on establishing routine production of high QE-films on a Mo substrate and demonstration of high average current and low transverse momentum. This work is carried out in a lab dedicated to photocathode production and characterization. The latter consists of measurements of QE as a function of energy, reflectivity, scattering, and angle-resolved photoemission for momentum measurements. While we believe that K_2CsSb is the ideal material, it is unproven under our precise conditions of QE and emittance, and so we also plan to investigate Cs_2Te as used at FLASH as a backup option [20]. This material, although now proven to achieve high QE and long lifetime, requires significantly higher laser power due to its UV threshold.

VHF photo gun

To meet the needs of a future high-repetition-rate FEL facility, LBNL is developing a VHF CW laser photocathode rf gun using a room-temperature copper cavity. This project has the potential to significantly influence the design of either a high repetition-rate linac-based FEL or an energy-recovery linac. Major performance goals are listed in Table 2; flexibility and reliability in operation are additional key factors influencing our design. Simultaneously satisfying these performance parameters allows us to achieve two main goals—production of the high-brightness beam required by the FEL and the capability to operate with high-QE photocathodes requiring extremely low vacuum pressures. This last requirement is necessary for operating at high repetition rate with present laser technology. We chose a room-temperature CW VHF cavity with laser photocathode to meet all the performance parameters simultaneously. The use of mature and robust VHF cavity technology overcomes the reliability challenges of other techniques while accommodating a variety of cathode materials and allowing a high accelerating gradient at the cathode at high repetition rate [21, 22, 23, 24]. Preliminary beam dynamics studies show the capability of such a gun to generate the beam parameters required to operate a soft X-ray FEL [25].

The core of such a gun is a normal-conducting rf cavity resonating at approximately 187 MHz. The frequency choice is compatible with both 1.3 and 1.5 GHz superconducting linac technologies, the most probable candidates for the main linac. Because of the low frequency, the structure is relatively large and the power density on the walls is small and compatible with CW operation using conventional water-cooling. Additionally, the long rf wavelength allows for the large high-conductance vacuum ports necessary for achieving the desired vacuum pressure. Figure 5 shows a cross section of the VHF cavity. Most of the cavity is made of solid OFHC copper externally supported by stainless steel flanges. Çooling channels are machined into areas of highest heat load, and cooling tubes provided for other areas. The vacuum system is designed to achieve a pressure into the low 10^{-11} Torr range when operating at the nominal rf power.

The VHF cavity is currently under construction, and the VHF tetrode power supply is being procured from a commercial supplier. Preparation of the shielded area for housing the photoinjector has started, and initial rf conditioning followed by tests of gradient and vacuum conditions are planned for 2010.

Timing and synchronization systems

LBNL staff are developing timing distribution systems for synchronization of rf plants and/or lasers in short-pulse FEL facilities [26, 27, 28]. Currently we are prototyping a timing system that will synchronize pulsed lasers to the electron-bunch arrival time in the LCLS, and another system that will deliver a stable rf reference to the low-level rf system in the FERMI@Elettra FEL at Sincrotrone Trieste. The scheme used for both systems is to modulate S-band rf (~3 GHz) onto a single-frequency, wavelength-stabilized laser signal delivered over fiber optics and to receive the rf on a photodiode. Changes in fiber length are monitored by an interferometer that uses the same laser signal and provides information to a digital phase shifter at the receiver. The received rf is digitized and numerically phase shifted in proportion to the interferometer data on fiber length. This phase-shifted signal can be compared with a local oscillator or with a pickup from an accelerating cavity to generate an error signal for control [29]. All components are standard fiber telecom, microwave, and digital parts, built into rackmount chassis. The transmitter equipment fits in a standard 6-ft-high rack, while the receiver is a chassis with a remote phase sensor connected by delay-corrected cables. The sensor can be located near a laser or an accelerator cavity, to minimize uncorrected cable length.

Tests have been made of a dual-channel transmitter/receiver set with different fiber lengths in the two channels. As shown in Figure 6, the relative rms temporal stability over 60 h was 19.4 fs with 2.2 km in one channel and 2 m in the other. With 200 m in one channel and 2 m in the other, the rms stability over 20 h was 8.4 fs. Currently we have replaced the dual-channel receiver with two single-channel receivers, one controlling a voltage-controlled oscillator. Preliminary tests show about 20-fs relative stability over 12 h, with 200 m of fiber in one channel. Specifications are 50 fs rms for FERMI@Elettra and 100 fs for LCLS, both requiring about 200-m fiber runs, so we will be able to meet these with some margin.

Summary

LBNL is developing a design concept for a soft X-ray free-electron laser light source with capabilities of extreme spatial, temporal, and energy resolution, which would serve a broad community of research scientists and engineers in many fields. We are embarked on a research, development and design program addressing the most critical needs of photocathodes and gun

design aimed at the demonstration of high-brightness, high-rep-rate capability, beam delivery and FEL design concepts, and timing and synchronization systems for ultrafast pump-probe experimentation. Together with collaborations and developments in FEL technologies pursued at other institutions, these activities will form the basis for a SXR FEL facility design offering truly unique capabilities.

Acknowledgments

The authors gratefully acknowledge helpful contributions from G. Stupakov and D. Xiang at SLAC for their assistance with FEL design studies.

References

1. U.S. Department of Energy (US DOE), Basic Energy Sciences Advisory Committee (BESAC), "New Science for a Secure and Sustainable Energy Future," http://www.sc.doe.gov/bes/reports/list.html (2008).
2. US DOE BESAC, "Next-Generation Photon Sources for Grand Challenges in Science and Energy," http://www.sc.doe.gov/bes/reports/list.html (2009).
3. US DOE BESAC, "Directing Matter and Energy: Five Challenges for Science and the Imagination," http://www.sc.doe.gov/bes/reports/list.html (2007).
4. Argonne National Laboratory, Brookhaven National Laboratory, Lawrence Berkeley National Laboratory, and SLAC National Accelerator Laboratory, "Science and Technology of Future Light Sources," http://www.als.lbl.gov/als/publications/genpubs.html (2008).
5. Lawrence Berkeley National Laboratory, "Toward Control of Matter: Energy Science Needs for a New Class of X-Ray Light Sources," https://hpcrd.lbl.gov/sxls/home.html (2008).
6. A. Belkacem et al., *Synchrotron Radiation News* **20**, 20 (2007).
7. R. Brinkman et al., "TESLA Technical Design Report Part II," http://tesla.desy.de/new_pages/TDR_CD/PartII/accel.html (2001).
8. A .A. Zholents et al., *Proc. LINAC08*, paper TUP046 (2008).
9. E. L. Saldin et al., *Nucl. Instrum. Methods Phys. Res., Sect. A* **490**, 1 (2002); E. L. Saldin et al., TESLA FEL- 2003-02 (2003).
10. M. Venturini, *Phys. Rev. ST Accel. Beams* **10**, 104401 (2007).
11. A.A. Zholents et al., "Design of the electron beam switch yard for an array of Free Electron Lasers," CBP Tech. Note 401 (March 2009).
12. Z. Huang et al., *Phys. Rev. ST Accel. Beams* **7**, 074401 (2004).
13. J. Qiang et al., *J. Comp. Phys* **163**, 434 (2001).
14. S. Heifets et al., *Phys. Rev. ST Accel. Beams* **5**, 064401 (2002).
15. G. Stupakov, *Phys. Rev. Lett.* **102**, 074801 (2009).
16. D. Xiang and G. Stupakov, "Coherent soft X-ray generation in the water window with the EEHG scheme," *Proc. PAC09* (2009).
17. I. V. Schweigert and S. Mukamel, *Phys. Rev. A* **76**, 01250 (2007).
18. A. Zholents and G. Penn, "Obtaining two attosecond pulses for X-ray stimulated Raman spectroscopy," CBP Tech. Note 403 (May 2009).
19. D. H. Dowell et al., *Nucl. Instrum. Methods Phys. Res., Sect. A* **356**, 167 (1995).

20. P. Michelato et al., *Nucl. Instrum. Methods Phys. Res., Sect. A* **393**, 464 (1997); Lederer et al., *Proc. EPAC08*, paper MOPC072 (2008).
21. C. Hernandez-Garcia et al., *Proc. FEL04*, paper TUPOS61 (2004).
22. J. Staples et al., *Proc. EPAC04*, paper MOPKF069 (2004).
23. J. Staples et al., "VHF-band photoinjector," CBP Tech. Note 366 (October 2006).
24. K. Baptiste et al., *Nucl. Instrum. Methods Phys. Res., Sect. A* **599**, 9 (2009).
25. K. Baptiste et al., "Status of the LBNL normal-conducting CW VHF photo-injector," *Proc. PAC09* (2009).
26. R. B. Wilcox et al., *Proc. PAC05*, paper RPAT075 (2005).
27. R. B. Wilcox and J. W. Staples, *Proc. PAC07*, paper FROAC05 (2007).
28. R. B. Wilcox and J. W. Staples, *Proc. CLEO 2007*, paper CThHH4 (2007).
29. J. W. Staples et al., *Proc. LINAC08*, paper THP118 (2008).

Table 1: Performance goals for a future seeded FEL facility.

	Ultrashort-pulse beamlines	**Short-pulse beamlines**	**High-spectral-resolution beamlines**
Pulse length (fs)	0.3–10	10–100	100–500
Wavelength range (nm)	1–30	1–100	1–100
Repetition rate (kHz)	1–10 (goal 100)	100	100
Peak power (GW)	0.1–1	0.1–5	0.1–5
Photons/pulse (@ 1 nm)	1.5×10^8 (0.3 fs, 0.1 GW)	5×10^{11} (100 fs, 1 GW)	2.5×10^{12} (500 fs, 1 GW)
Bandwidth	Fourier transform limit (FTL)	few x FTL	few x FTL
Photons/pulse (@ 3rd harmonic 0.3 nm)	2×10^6 (in 100 as)	2×10^9 (in 100 fs)	2×10^{10} (in 500 fs)
Polarization	Variable, linear/circular	Variable, linear/circular	Variable, linear/circular
Peak brightness (@ 1 nm) (ph/s/mm^2/mr^2/0.1%BW)	$\sim 10^{30}$	$\sim 10^{33}$	$\sim 10^{34}$
Average brightness (@ 1 nm) (ph/s/mm^2/mr^2/0.1%BW)	$\sim 10^{19}$ (10 kHz)	$\sim 10^{25}$	$\sim 10^{27}$

Table 2. CW photocathode gun VHF cavity main parameters.

Total length (m)	0.35
Cavity internal diameter (m)	0.694
Accelerating gap (mm)	40
Frequency (MHz)	187
Q_0	31000
Pulse rate	CW
Gap voltage (MV)	0.75
Electric field at the cathode (MV/m)	19.5
Peak surface electric field (MV/m)	24.1
Shunt impedance (MW)	6.5
RF power for 0.75 MV at Q_0 (kW)	87.5
Peak wall power density at 0.75 MV (W/cm^2)	25.0

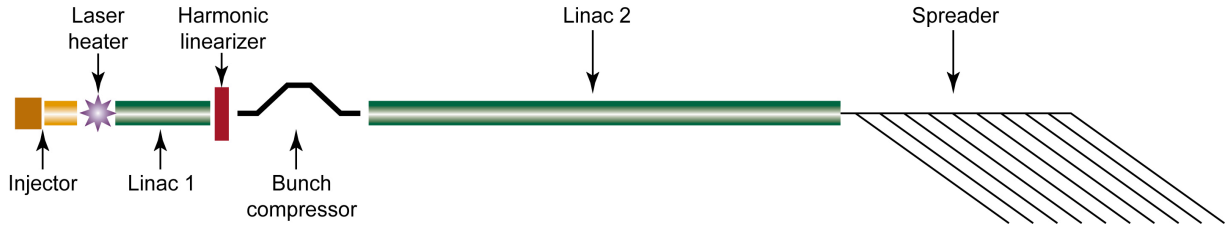

Figure 1: A schematic of the accelerator layout. The entire length of the machine is about 650 m.

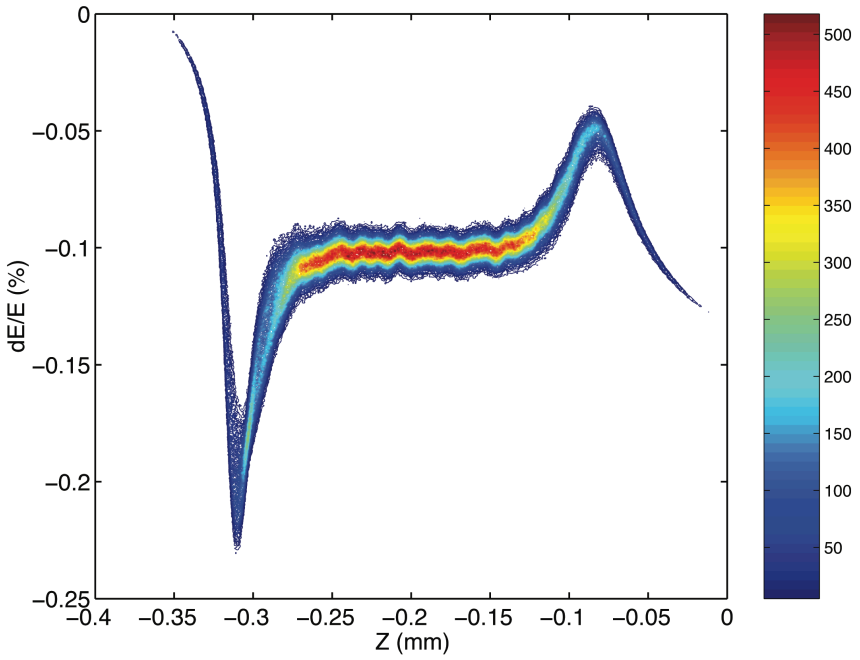

Figure 2: Density plot of the longitudinal phase space at the end of the spreader obtained in tracking five billion macroparticles through the entire machine beginning from the end of the injector using computer code IMPACT. The energy modulation with approximately 15-μm period seen here is in a good agreement with the analytical estimate of the microbunching instability based on a linear model.

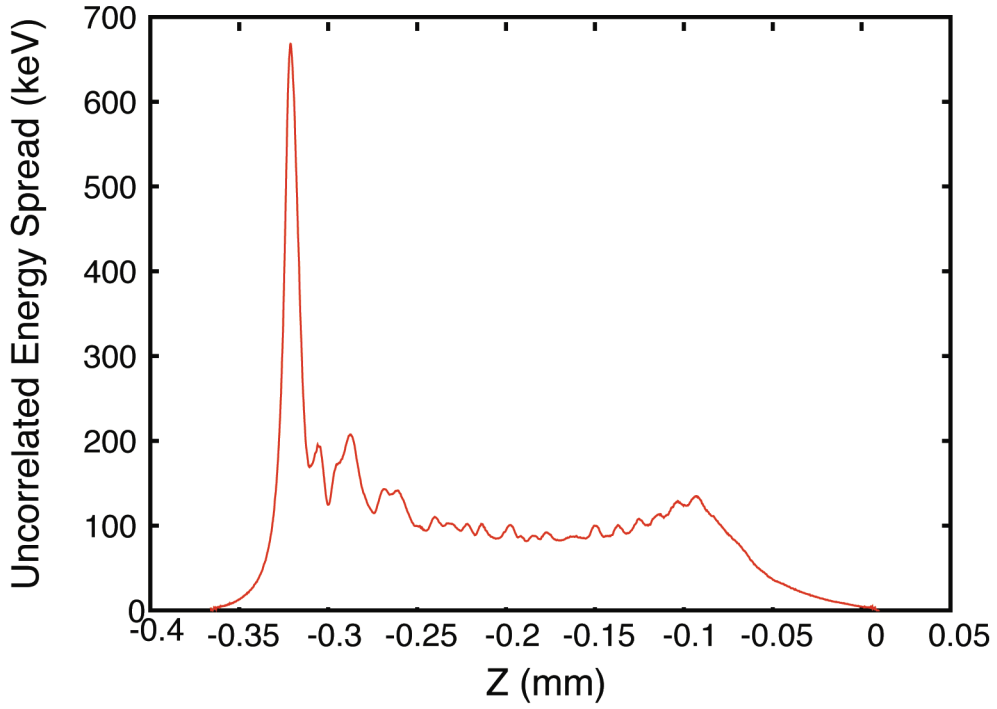

Figure 3: Slice rms energy spread at the end of the spreader obtained in tracking five billion macroparticles through the entire machine beginning from the end of the injector using computer code IMPACT. Large values at the left are due to correlated energy variations seen in Figure 2 that affected the rms value.

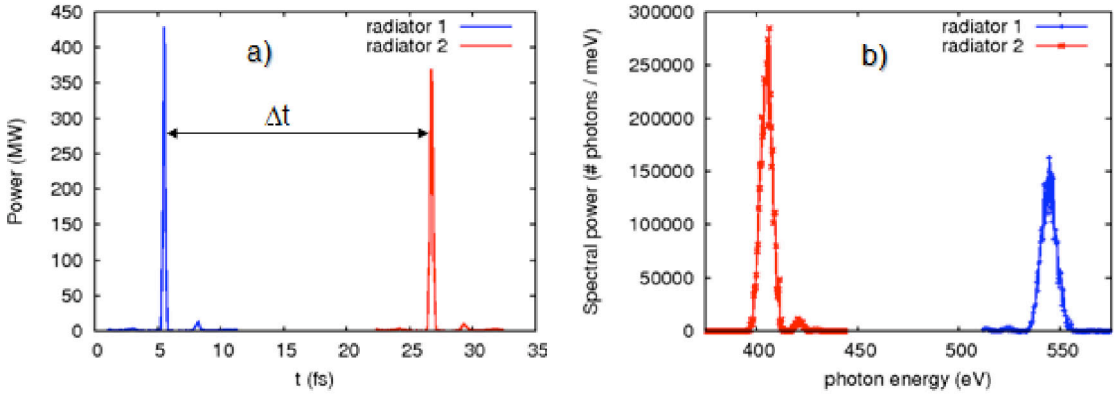

Figure 4: Possible ultrafast pulse pair with variable delay, according to the scheme described in [18]. (a) Pulse intensity. The FWHM pulse widths are 220 asec (blue) and 260 asec (red). We note that the time delay between the two pulses can be controlled with ultimate precision as both pulses originated from the same parent pulse. (b) Spectral power. The FWHM pulse widths are 6.6 eV (red) and 8.6 eV (blue).

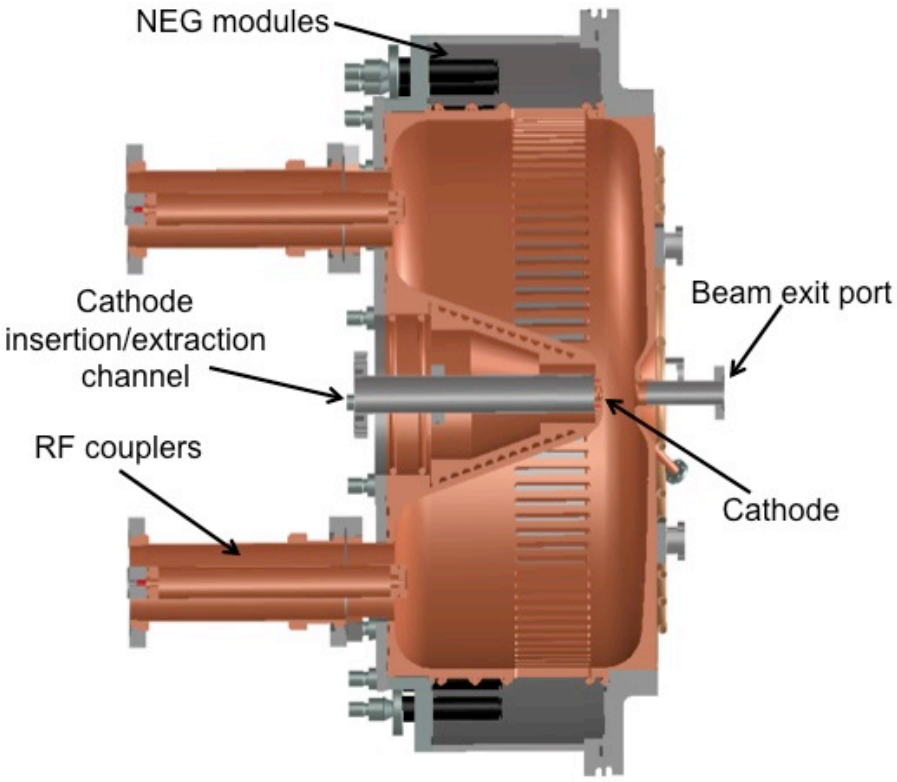

Figure 5: CW photocathode gun VHF cavity in cross section, showing major components.

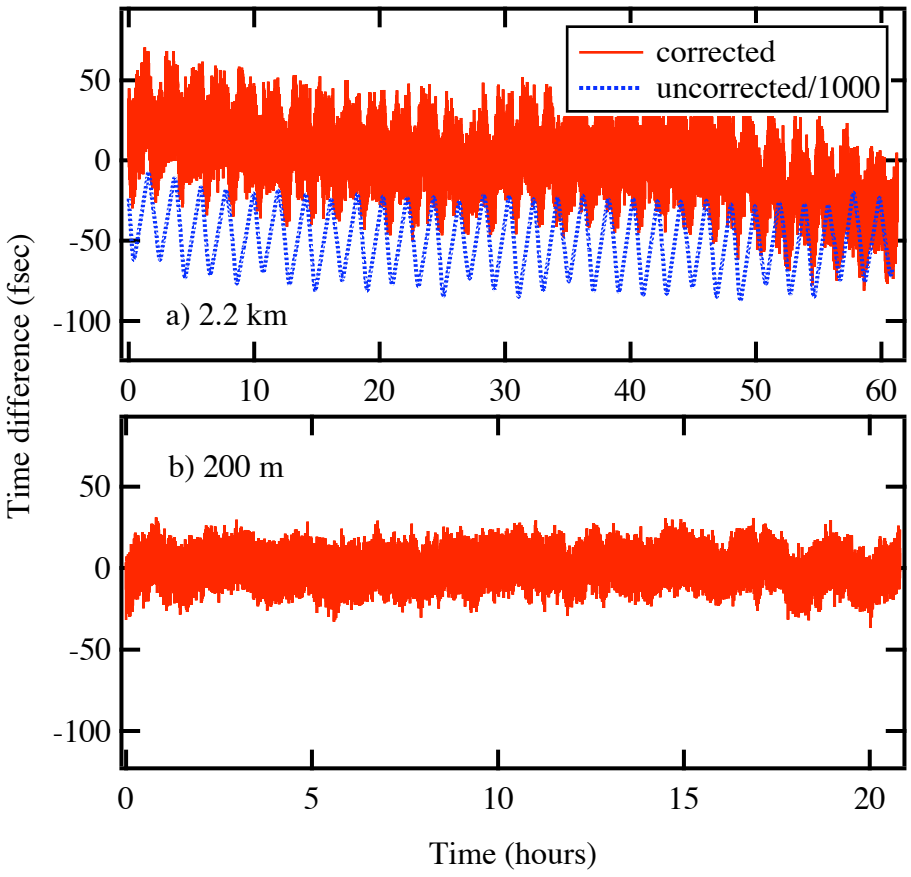

Figure 6: Relative drift of a 2850-MHz signal transmitted over a long (2 km) and short (2 m) fiber. (a) 2.2-km fiber. The relative time difference has a 19.4-fs rms deviation over 60 h. The relative time difference (/1000) without the correction is also shown. (b) A 200-m fiber has an 8.4-fs rms deviation over 20 h.